MATEMATIKA, MJIAM, Volume 42, Number 2, 221–248

Backward Bifurcation in a Mathematical Model of Drug-Resistance Tuberculosis

[1,2]Usman Garba, [1]Amirah Azmi* and [1]Mohd Hafiz Mohd

[1]School of Mathematical Sciences, Universiti Sains Malaysia, 11800 Minden, Pulau Pinang, Malaysia.
[2]Department of Mathematics/Computer, College of Education Billiri, Gombe State, Nigeria.
*Corresponding author: amirahazmi@usm.my

Article history
Received: 24 January 2024
Received in revised form: 24 March 2025
Accepted: 23 April 2025
Published online: 20 July 2026

Abstract This study focuses on the proliferation of tuberculosis, a contagious condition caused by *Bacillus Mycobacterium*, with particular emphasis on its effects on drug-resistant individuals. Tuberculosis treatment typically lasts 6–8 months for newly infected individuals and can extend up to 2.5 years for patients with multidrug resistance. Despite decades of research, the widespread use of a vaccine, and the seeming attempt by the WHO to support a single worldwide management approach in recent years, TB is the second most common infectious killer, behind COVID-19. A projected 10.8 million persons worldwide contracted tuberculosis (TB) in 2023, either latently or actively. The dynamics of tuberculosis transmission among the human population are examined using a mathematical model that considers two subgroups: primary infectious and drug-resistant individuals. The basic reproduction number was established, and the model underwent sensitivity analysis to identify the primary variables affecting the disease's transmission. The findings of this analysis can aid in proposing effective intervention strategies. This study investigated the TB endemic equilibrium point and evaluated the global and local stability associated with the TB disease-free equilibrium point. First, we examined how the transmission rate impacted the model's backward bifurcation. According to our findings, the model experiences a backward bifurcation as the transmission rate increases. Complete eradication of TB becomes unattainable within the range of a scaling factor between 2.53 and 2.13. Second, we investigated the effect of the recovery rate among individuals who developed drug resistance on the backward bifurcation of the model. Our results show that the model exhibits a back bifurcation when the recovery rate rises. The bifurcation changes backward to forward when the transmission rate's scaling factor values go from 0.5 to 1. Stable disease-free equilibrium (DFE) and stable endemic equilibria coexist globally. Based on these observations, we conclude that the drug-resistance compartment is a more significant concern than the infected class, highlighting the need for vigilance among health workers and government agencies in monitoring this silent source of tuberculosis transmission.

Keywords Tuberculosis; Drug-resistance; Bi-quadratic polynomial.

Mathematics Subject Classification 00A71.

1 Introduction

The infectious disease known as tuberculosis (TB) is caused by *Mycobacterium tuberculosis*. The respiratory system, specifically the lungs, is primarily affected [1]. Nevertheless, various organs may be harmed., including the lymphatic system, kidneys, spine, brain, and central nervous system [2,3]. Active lung TB is characterized by symptoms such as persistent cough, sometimes accompanied by sputum or blood, fatigue, weight loss, fever, and night sweats persisting for at least three weeks. In 2023, there were 10.8 million cases of tuberculosis recorded globally, with 1.2 million cases in children and 9.4 million cases in adults [4]. In 2023, 55% of tuberculosis cases were male, 33% were female, and 12% were children and young adolescents. The global number of tuberculosis deaths declined in 2023, continuing the decline in 2022 following two years of increases during the worst years of the COVID-19 epidemic (2020 and 2021) [4]. In 2023, tuberculosis was expected to cause 1.25 million deaths (95% UI: 1.13-1.37 million), with 1.09 million among HIV-negative persons and 161,000 among HIV-positive people. The total was lower than the best predictions of 1.32 million in 2022, 1.42 million in 2021, and 1.40 million in 2020, and fell below the pre-pandemic level of 1.34 million in 2019 [4]. Despite this development, tuberculosis is likely to return as the world's most significant cause of death from a single infectious agent (replacing COVID-19). Globally, 8.2 million persons were recorded as newly diagnosed with tuberculosis in 2023, up from 7.5 million in 2022 and 7.1 million in 2019 and well beyond the estimates of 5.8 million in 2020 and 6.4 million in 2021 [4]. Those newly diagnosed in 2022 and 2023 likely included a sizable backlog of patients who contracted tuberculosis in prior years but had their diagnosis and treatment delayed due to COVID-related delays [4].

Backward bifurcations, which are characterized by multiple coexisting equilibria, allow a disease to persist even though$R_0 < 1$. More specifically, one can find a stable disease-free equilibrium coexisting with two endemic equilibria ($I > 0$) unstable and stable even though $R_0 < 1$. The presence of backward bifurcation is essential in a practical sense because control programs must reduce $R(0)$ further than below unity to eliminate a disease [5].

A mathematical model was created for the dynamics of TB transmission with reinfection [6]. This study focused on the boundedness of the TB model incorporating reinfection and identified a biologically meaningful region for its solutions. Through mathematical analysis, the researchers established that the TB model with reinfection exhibits local and global asymptotic stability under specific conditions. The model is stable when the basic reproductive number $R(0)$ is smaller than 1, leading to the disappearance of TB infection. Conversely, when $R(0)$ exceeds 1, the model remains stable, and TB infection persists. Numerical simulations corroborated the theoretical findings, revealing that higher reinfection rates elevate the force of infection, yet the infected population persists at equilibrium.

Das et al. [7] developed an SEIR pandemic TB transmission model focusing on control measures. Two stability points were identified: both an endemic and an infection-free equilibrium. When the number of reproductions is smaller than one, the infected population decreases toward infection-free equilibrium, whereas reproduction numbers exceeding one lead to oscillations and disease persistence. A transcritical bifurcation occurs at a reproduction number of one. Furthermore, the disease is globally asymptotically stable and eliminated from the system if there is an endemic equilibrium.

In [8], a mathematical simulation of the mechanics of TB transmission was developed to study the effect of multidrug-resistant and vaccinated individuals. In their study, vaccination and quarantine classes were considered. They obtained the thresholds and equilibrium of the system. They also received the model system's reproduction number and stability. After all, they performed a simulation and discovered that quarantining TB patients with multiple medication resistance recovered quickly and almost completely prevented the spread of the TB virus. By immunizing TB patients, they found that vaccination would decrease the number of active TB cases. [9] created a five-compartmental model of TB that is deterministic to study the impact of quarantining multidrug-resistant tuberculosis (MDR-TB) individuals. Their model system exhibits two equilibria that lead to backward bifurcation. The numerical simulation provides a visual depiction of how implementing quarantine measures can successfully lower disease prevalence and manage instances of multidrug-resistant tuberculosis (MDR-TB).

However, in their model, the authors of [6,7,10–12] excluded individuals who developed drug resistance. One of the crucial elements in individuals' lives is still this factor. The provision of public health services played a role in decreasing the transmission of tuberculosis. Taking cues from earlier conversations, the objective of this article is to address a deficiency in the sources referred to by considering individuals who are both presently infected and resistant to drugs. This work aimed to explore theoretical and numerical solutions while examining the effects of medication resistance. To achieve this goal, we used the widely recognized S, E, I, I_R, R model.

This article is structured into five distinct sections. Section 2 outlines the dynamic TB model, focusing on drug resistance. Besides, in this section, we also examine the solution's existence, uniqueness, and positivity and invariant region for S, E, I, I_R, the R and dynamics models. After that, Section 3 presents the theoretical analysis of the nonlinear model, including the determination of equilibrium points and the investigation of its local and global stability. Furthermore, the section discusses the bifurcation analysis and sensitivity analysis to provide a comprehensive understanding of the model dynamics. Section 4 then provides numerical solutions and corresponding simulations to validate our findings. Our concluding remarks and the study's findings are presented in section 5.

2 Mathematical Model Formulation

This article focuses on a TB model that considers drug-resistance and reinfection among individuals who have previously undergone treatment. The model is a modification of existing TB transmission models developed by researchers [6,7,10–12]. The modification expands upon the model proposed by [6] by incorporating a new class for drug-resistant individuals, resulting in a model represented as $SEII_RRE$. The inclusion of the drug-resistance class is crucial because drug-resistant TB is considered the most dangerous form of the disease. The modified model also shares similarities with the one developed by [6] but differs in times of variables. The researchers aim to create a more comprehensive and realistic TB transmission model that better captures the complexities of the disease, particularly when considering drug-resistant cases and reinfection among treated individuals. The development of such models is essential for improving our understanding of TB dynamics and guiding effective strategies for disease control and prevention. We take into account the entire population of humans, symbolized as $N(t)$, which is further separated into six sections that are mutually exclusive: susceptible individuals $S(t)$, latently infected individuals $E(t)$, primary infectious individuals $I(t)$, infected individuals who

developed drug resistance $I_R(t)$, and recovered individuals with temporary immunity $R(t)$ as shown in Figure 1. By bringing new people into the population through births at a steady rate π, the susceptible compartment is enlarged and a natural death decreases each subpopulation at a rate μ. The susceptible individuals get the infection at the rate of $\lambda = \dfrac{\beta(I + \rho I_R)}{N}$ known as standard incidence. At a rate of κ , those who have been exposed advance to the major infectious class. primary infectious individuals recovered at the rate τ , reduced as a related mortality a rate δ_1 and progressed to the drug-resistance class due to failure to complete an entire course of TB treatment at the σ. The rate of recovery for drug-resistant people was while the rate of decline was δ_2, because of TB-related death. Lastly, the recovered people may become infected again due to low immunity; but with a lower level at the $(1 - \psi)$.

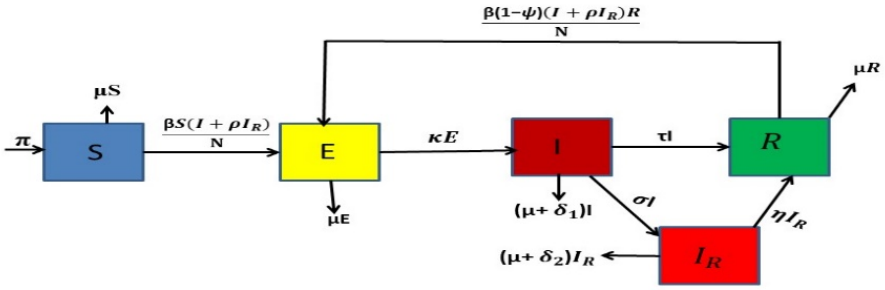

Figure 1: Flow diagram of the tuberculosis model

2.1 Clinical Assumptions of the Tuberculosis (TB) Model with Drug-Resistance and Reinfection

The model's fundamental biological presumptions are as follows.

1. The susceptible population is continuously recruited, and people in all compartments die from natural causes in addition to an additional death rate exclusively linked to tuberculosis infection within the infected class [10].
2. The population transitioning from the susceptible to the infected class is considered a standard incidence, represented as "$\dfrac{\beta(I + \rho I_R(t)}{N}$" in its mathematical form [10].
3. An individual who has recovered might be susceptible to reinfection by an infectious person [10].
4. To maintain simplicity, it should be noted that in this context, we are not distinguishing between individuals infected by different strains.

2.2 Model Equations

The model comprises a set of nonlinear ODEs

$$\left.\begin{aligned}
\frac{dS}{dt} &= \pi - \left(\frac{\beta(I+\rho I_R)}{N} + \mu\right) S, \\
\frac{dE}{dt} &= \frac{\beta(I+\rho I_R)S}{N} + \frac{\beta(1-\psi)(I+\rho I_R)R}{N} - (\kappa+\mu)E, \\
\frac{dI}{dt} &= \kappa E - (\tau+\sigma+\delta_1+\mu)\, I, \\
\frac{dI_R}{dt} &= \sigma I - (\eta+\delta_2+\mu)\, I_R, \\
\frac{dR}{dt} &= \tau I + \eta I_R - \left(\frac{\beta(1-\psi)(I+\rho I_R)}{N} + \mu\right) R.
\end{aligned}\right\} \tag{1}$$

The system is considered with the initial conditions

$$S(0) \geq 0, \quad E(0) \geq 0, \quad I(0) \geq 0, \quad I_R(0) \geq 0, \quad R(0) \geq 0,$$

where

$$\big(S(0), E(0), I(0), I_R(0), R(0)\big) \in \mathbb{R}^5_+ \setminus \{\mathbf{0}\},$$

and

$$N = S + E + I + I_R + R.$$

Furthermore,

$$\Sigma = \frac{\beta(I+\rho I_R)}{N}. \tag{2}$$

The force of infection, represented by equation (2), allows the rewriting of model system (1) as

$$\left.\begin{aligned}
\frac{dS}{dt} &= \pi - (\Sigma+\mu)\, S, \\
\frac{dE}{dt} &= \Sigma S + \Sigma(1-\psi)R - (\kappa+\mu)E, \\
\frac{dI}{dt} &= \kappa E - (\tau+\sigma+\delta_1+\mu)\, I, \\
\frac{dI_R}{dt} &= \sigma I - (\eta+\delta_2+\mu)\, I_R, \\
\frac{dR}{dt} &= \tau I + \eta I_R - (\Sigma(1-\psi)+\mu)\, R.
\end{aligned}\right\} \tag{3}$$

Table 1 provides the numerical values and corresponding sources for the key parameters governing the flow between model (1) compartments.

Table 1: Model parameters

Parameter	Description	Value	Source
π	Rate of Recruitment	450862	[2]
ψ	The rate of low immunity in recovered individuals	0.8	Assumed
β	Transmission Rate	2.53	[3]
κ	The rate at which the exposed class advances to become the primary infectious class	0.1196	[4]
ρ	Modification parameters associated with drug-resistance in individuals	0.85	Assumed
σ	Progression rate of primary infectious individuals into the drug resistance class	0.02	Assumed
η	Transitioning from the drug-resistant class to the recovered class	0.5	[3]
τ	Individuals' progression from the primary infectious class to the recovered class	2.0	[13]
δ_1	Death rate due to primary infectious TB individuals	0.19	[3]

2.3 Basic Properties of the Model

The essential features of the TB model are examined in this section. Considering the mathematical presentation in equation set (1), which illustrates the fluctuations in various segments of the populations, its epidemiological significance lies in ensuring that all state variables remain non-negative throughout time $t > 0$. To clarify, the solutions derived from (1), given initial data with positive values, will consistently maintain positivity for all time values greater than zero. It is important to emphasize that because the model encapsulates the interplay between populations, It is assumed that every model parameter has a value that is not negative. Consequently, the ensuring outcome is as follows.

2.3.1 Existence and uniqueness

Theorem 1. Let

$$X(t) = \big(S(t), E(t), I(t), I_R(t), R(t)\big) \in \mathbb{R}^5_+,$$

where

$$\mathbb{R}^5_+ = \{X = (S, E, I, I_R, R) : S, E, I, I_R, R \geq 0\}.$$

Assume that all model parameters are positive constants and that $N > 0$. If the vector field $f : \Omega \subset \mathbb{R}^5_+ \to \mathbb{R}^5$ associated with system *(1)* is continuously differentiable on the region

$$\Omega = \big\{X \in \mathbb{R}^5_+ : 0 \leq N \leq K\big\},$$

for some positive constant K, then f is locally Lipschitz continuous on Ω. Consequently, for every nonnegative initial condition

$$X(0) = \big(S(0), E(0), I(0), I_R(0), R(0)\big) \in \mathbb{R}^5_+,$$

system (1) admits a unique local solution.

Proof: To prove the existence and uniqueness of solution, we express the model (1) as

$$\frac{\partial X}{\partial t} = f(X) \tag{4}$$

where f is Lipschitz continuous function, while $X = (S, E, I, I_R, R)$. It follows from [14] that the model (1) has a unique solution, whenever the initial conditions are nonnegative. Let $x_1 = S, x_2 = E, x_3 = I, x_4 = I_R$ and $x_5 = R$. Also f_1, f_2, f_3, f_4, f_5 be respectively, the equations in (1), as follows.

$$\left.\begin{aligned}
f_1 &= \pi - \left(\frac{\beta(x_3 + \rho x_4)}{N} + \mu\right) x_1, \\
f_2 &= \frac{\beta(x_3 + \rho x_4)x_1}{N} + \frac{\beta(1-\psi)(x_3 + \rho x_4)x_5}{N} - (\kappa + \mu)x_2, \\
f_3 &= \kappa x_2 - (\tau + \sigma + \delta_1 + \mu)x_3, \\
f_4 &= \sigma x_3 - (\eta + \delta_2 + \mu)x_4, \\
f_5 &= \tau x_3 + \eta x_4 - \left(\frac{\beta(1-\psi)(x_3 + \rho x_4)}{N} + \mu\right) x_5.
\end{aligned}\right\} \tag{5}$$

Our goal is to show that $\dfrac{\partial f_i}{\partial t} i = 1, 2, 3, 4, 5$ are continuous and bounded in d. Now, from (5)

$$\begin{aligned}
&\left|\frac{\partial f_1}{\partial x_1}\right| = \left|-\left(\frac{\beta(x_3 + \rho x_4)}{N} + \mu\right)\right| < \infty, \quad \left|\frac{\partial f_1}{\partial x_3}\right| = \left|-\frac{\beta x_1}{N}\right| < \infty, \quad \left|\frac{\partial f_1}{\partial x_4}\right| = \left|-\frac{\beta \rho x_1}{N}\right| < \infty, \\
&\left|\frac{\partial f_1}{\partial x_2}\right| = 0 < \infty, \quad \left|\frac{\partial f_1}{\partial x_5}\right| = 0 < \infty, \\
&\left|\frac{\partial f_2}{\partial x_1}\right| = \left|\frac{\beta(x_3 + \rho x_4)}{N}\right| < \infty, \quad \left|\frac{\partial f_2}{\partial x_2}\right| = |-(\kappa + \mu)| < \infty, \\
&\left|\frac{\partial f_2}{\partial x_3}\right| = \left|\frac{\beta(x_1 + (1-\psi)x_5)}{N}\right| < \infty, \quad \left|\frac{\partial f_2}{\partial x_4}\right| = \left|\frac{\beta\rho(x_1 + (1-\psi)x_5)}{N}\right| < \infty, \\
&\left|\frac{\partial f_2}{\partial x_5}\right| = 0 < \infty.
\end{aligned}$$

Similarly, the boundedness and continuity of the partial derivatives of f_3, f_4, and f_5 demonstrate that the vector field satisfies the Lipschitz condition. Therefore, if the initial conditions are nonnegative, system (1) admits a unique solution in $\mathbb{R}^5_+$.

2.3.2 Positivity of the solution

Theorem 2. Let $S(t) \geq 0, E(t) \geq 0, I(t) \geq 0, I_R(t) \geq 0, R(t) \geq 0$ be the initial data for TB (1). Then the solutions $(S(t), E(t), I(t), I_R(t), R(t))$ of the model with positive initial data, will remain positive for all time $t > 0$.

Proof: Let t_η denote the supremum of all positive times such that the solution remains positive for every $s \in [0,t]$, that is,

$$t_\eta = \sup\left\{t > 0 : S(s) > 0,\ E(s) > 0,\ I(s) > 0,\ I_R(s) > 0,\ R(s) > 0,\ \forall s \in [0,t]\right\}.$$

Hence, $t_\eta > 0$. Then, model system (3) indicates

$$\frac{dS}{dS} = \pi - (\lambda + \mu)S.$$

The above equation can be written using the integrating factor method, as follow.

$$\begin{aligned}
\frac{d}{dt}\left[S(t)\exp\left\{\mu t + \int_0^t \lambda(k)\,dk\right\}\right] &\geq \pi \exp\left\{\mu t + \int_0^t \lambda(k)\,dk\right\},\\
S(t)\exp\left\{\mu t + \int_0^t \lambda(k)\,dk\right\} - S(0) &\geq \pi \int_0^t \exp\left\{\mu\varpi + \int_0^\varpi \lambda(k)\,dk\right\} d\varpi,\\
S(t)\exp\left\{\mu t + \int_0^t \lambda(k)\,dk\right\} &\geq S(0) + \pi \int_0^t \exp\left\{\mu\varpi + \int_0^\varpi \lambda(k)\,dk\right\} d\varpi,\\
S(t) &\geq S(0)\exp\left\{-\mu t - \int_0^t \lambda(k)\,dk\right\}\\
&\quad + \pi \exp\left\{-\mu t - \int_0^t \lambda(k)\,dk\right\} \int_0^t \exp\left\{\mu\varpi + \int_0^\varpi \lambda(k)\,dk\right\} d\varpi > 0.
\end{aligned}$$

The remaining state variables $V(t) \geq 0, E(t) \geq 0, I(t) \geq 0, I_R(t) \geq 0$ and $R(t) \geq 0$ behave similarly, where, they all have values of zero for any time $t \geq 0$. Therefore, for all non-negative initial circumstances, all solutions of model (3) stay positive.

2.3.3 Invariant region

Theorem 3. Let $S(t)$, $E(t)$, $I(t)$, $I_R(t)$, and $R(t)$ denote the state variables of system (1) with nonnegative initial conditions. The feasible region of the model is defined as

$$\Theta = \left\{(S(t), E(t), I(t), I_R(t), R(t)) \in \mathbb{R}_+^5 : N(t) \leq \frac{\pi}{\mu}\right\}, \tag{6}$$

where $N(t) = S(t) + E(t) + I(t) + I_R(t) + R(t)$. Then, the region Θ is positively invariant and the total population size $N(t)$ remains bounded. Moreover, if $N(0) < \dfrac{\pi}{\mu}$, then

$$N(t) \to \frac{\pi}{\mu} \quad \text{as} \quad t \to \infty,$$

indicating that $\dfrac{\pi}{\mu}$ is an asymptotically stable equilibrium point for the total population.

Proof: By adding all equations of the model system together, we obtain

$$\frac{dN}{dt} = \pi - \mu(S + E + I + I_R + R) - (\delta_1 I + \delta_2 I_R),$$

where $N = S + E + I + I_R + R$. For $t > 0$, the following inequality is obtained.

$$\frac{dN}{dt} \leq \pi - \mu N. \tag{7}$$

By applying the comparison theorem presented in [8], it follows that

$$N(t) \leq \frac{\pi}{\mu}\left(1 - e^{-\mu t}\right) + N(0)e^{-\mu t}. \tag{8}$$

As shown in [8], if $N(0) < \dfrac{\pi}{\mu}$, then

$$N(t) \to \frac{\pi}{\mu} \quad \text{as} \quad t \to \infty.$$

Hence, the equilibrium point $\dfrac{\pi}{\mu}$ is asymptotically stable, and the total population satisfies

$$0 \leq N(t) \leq \frac{\pi}{\mu}.$$

Therefore, the feasible region Θ is positively invariant.

The fundamental model is well articulated, both epidemiologically and mathematically. Therefore, studying the dynamics of the fundamental model will suffice.

2.4 Basic Reproduction Number

The basic reproduction number is a threshold statistic that assesses the transmission of illness in a given population. Epidemiologically, it measures the average number of secondary infections that a single infected person can cause in a community that is entirely susceptible. In other words, the threshold quantity $R(0)$ in (10) represents the average number of tuberculosis infections that a tuberculosis-infected individual can cause in a completely susceptible population. To compute $R(0)$, we use the method of next generation matrix developed in [7, 15]. The non-negative matrix, F, of the new infection terms and the matrix V, of the transmission terms associated with the model (1) are given, respectively, by

$$F = \begin{bmatrix} 0 & \beta & \beta_\rho \\ 0 & 0 & 0 \\ 0 & 0 & 0 \end{bmatrix}, \qquad V = \begin{bmatrix} B_1 & 0 & 0 \\ -\kappa & B_2 & 0 \\ 0 & -\sigma & B_3 \end{bmatrix}. \tag{9}$$

This gives

$$FV^{-1} = \begin{bmatrix} \dfrac{\beta\kappa}{B_1B_2} + \dfrac{\beta\kappa\rho\sigma}{B_1B_2B_3} & \dfrac{\beta}{B_2} + \dfrac{\beta\kappa\rho\sigma}{B_1B_2B_3} & \dfrac{\beta\rho}{B_3} \\ 0 & 0 & 0 \\ 0 & 0 & 0 \end{bmatrix}.$$

The characteristic equation is obtained by solving

$$\left|FV^{-1} - \lambda I\right| = 0$$

which will result the eigenvalues

$$\lambda_1 = \lambda_2 = 0, \qquad \lambda_3 = \frac{\beta\kappa(B_3 + \rho\sigma)}{B_1B_2B_3} = \frac{\beta\kappa(\eta + \delta_2 + \mu + \rho\sigma)}{(\kappa + \mu)(\tau + \sigma + \delta_1 + \mu)(\eta + \delta_2 + \mu)},$$

where $B_1 = (\kappa + \mu), B_2 = (\tau + \sigma + \delta_1 + u)$ and $B_3 = (\eta + \delta_2 + \mu)$. Thus, following [7, 15],

$$R(0) = \frac{\beta\kappa(\eta + \delta_2 + \mu + \rho\sigma)}{(\kappa + \mu)(\tau + \sigma + \delta_1 + \mu)(\eta + \delta_2 + \mu)}. \tag{10}$$

3 Mathematical Analysis of the Model

In this part, we undertake a thorough examination of model (1) by identifying steady-state solutions. This encompasses verifying the presence of two equilibria, one where there is no TB occurrence (referred to as the TB-free equilibrium), and another where the disease is endemic. As adopted by [9, 16], the unique TB-free equilibrium for Model (1) is

$$E_0 = (S, E, I, I_R, R) = \left(\frac{\pi}{\mu}, 0, 0, 0, 0\right). \tag{11}$$

In addition, we assess the stability of these equilibria at both local and global levels. Moreover, we explore the type of bifurcation demonstrated by the model.

3.1 Local Stability of TB-Free Equilibrium (TFE)

As adopted in [10–12], the model system's Jacobian matrix (1) serves as an example of the local stability of the DFE. The characteristic equation is then derived using the Jacobian matrix to produce the eigenvalue outcome.

Theorem 4. When $R_0 < 1$, the tuberculosis-free equilibrium (TFE) of system (1) is locally asymptotically stable.

Proof: To investigate the local stability of the tuberculosis-free equilibrium E_0, we consider the Jacobian matrix of system (1), given by

$$J(E_0) = \begin{bmatrix} -\mu & 0 & -\beta & -\beta\rho & 0 \\ 0 & -B_1 & \beta & \beta\rho & 0 \\ 0 & \kappa & -B_2 & 0 & 0 \\ 0 & 0 & \sigma & -B_3 & 0 \\ 0 & 0 & \tau & \eta & -\mu \end{bmatrix}, \tag{12}$$

where

$$B_1 = \kappa + \mu, \qquad B_2 = \tau + \sigma + \delta_1 + \mu, \qquad B_3 = \eta + \delta_2 + \mu.$$

Using *Scientific WorkPlace*, the characteristic equation of the Jacobian matrix simplifies to

$$\begin{aligned}(\lambda + \mu)^2 \Big[\lambda^3 + (B_1 + B_2 + B_3)\lambda^2 + (B_1B_2 + B_1B_3 + B_2B_3 - \beta\kappa)\,\lambda \\ + B_1B_2B_3 - \beta\kappa(B_3 + \rho\sigma)\Big] = 0.\end{aligned} \tag{13}$$

Hence, two eigenvalues are

$$\lambda_1 = \lambda_2 = -\mu,$$

while the remaining three eigenvalues are obtained from the cubic equation

$$\lambda^3 + (B_1 + B_2 + B_3)\lambda^2 + (B_1B_2 + B_1B_3 + B_2B_3 - \beta\kappa)\,\lambda + B_1B_2B_3 - \beta\kappa(B_3 + \rho\sigma) = 0. \tag{14}$$

Let $m_3\lambda^3+m_2\lambda^2+m_1\lambda+m_0=0$, where $m_3=1$, $m_2=B_1+B_2+B_3$, $m_1=B_1B_2+B_1B_3+B_2B_3-\beta\kappa$, and $m_0=B_1B_2B_3-\beta\kappa(B_3+\rho\sigma)=B_1B_2B_3(1-R_0)$.

According to the Routh–Hurwitz criterion [17–20], all roots of the cubic polynomial have negative real parts if $m_3>0$, $m_2>0$, $m_1>0$, $m_0>0$, and $m_2m_1>m_3m_0$.

Since $m_3=1>0$, $m_2=B_1+B_2+B_3>0$, and $m_0=B_1B_2B_3(1-R_0)>0$ whenever $R_0<1$, together with $(B_1+B_2+B_3)(B_1B_2+B_1B_3+B_2B_3-\beta\kappa)>B_1B_2B_3(1-R_0)$, all the Routh–Hurwitz conditions are satisfied. Therefore, the three roots of the cubic polynomial have negative real parts. Combining these with the two eigenvalues $\lambda_1=\lambda_2=-\mu<0$, all eigenvalues of the Jacobian matrix have negative real parts whenever $R_0<1$.

Hence, the tuberculosis-free equilibrium of system (1) is locally asymptotically stable.

3.2 Global Stability of the TFE Point

The disease-free equilibrium of model (1) under [12] condition is examined in this study to determine its global asymptotic stability. Consider a sample system presented in the form

$$\left.\begin{aligned}\frac{dX_r}{dt}&=F(X_r,Z_r),\\ \frac{dZ_r}{dt}&=G(X_r,Z_r),\qquad (X_r,0)=0.\end{aligned}\right\} \tag{15}$$

where $X_r=(S,V,R)$ and $Z_r=(E,I,I_R)$ with the component of $X_r\in\mathbb{R}^3$ denoting the uninfected population and the components of $Z\in\mathbb{R}^3$ denoting the infected population. The disease-free equilibrium is now denoted as $E_0=(X_r^0,0)$, where $X_0=\left(\frac{\pi}{\mu},0,0\right)$.

Now, in order to guarantee global asymptotic stability, the requirements listed below must be met.

$$\begin{aligned}H_1:&\quad \frac{dX_r}{dt}=F(X_r,0),\quad X_r^0 \text{ is globally asymptotically stable,}\\ H_2:&\quad G(X_r,Z)=PZ-G(X_r,Z_r),\quad G(X_r,Z_r)\geq 0,\quad \text{for } (X_r,Z_r)\in\Omega,\end{aligned}$$

where $P=D_zG(X_r^0,0)$ is a M-matrix where the region of P represents the biologically plausible region of the model (the off-diagonal elements E^0 are non-negative). Given that $R_0<1$, E_0 is shown to be globally asymptotically stable by following [17] and this is stated in the next theorem.

Theorem 5. The disease-free equilibrium point $E_0=(X^*,0)$ of model system (1) is globally asymptotically stable if $R_0<1$ and the sufficient conditions (H_1) and (H_2) are satisfied.

Proof: To investigate the global stability of the disease-free equilibrium, the conditions (H_1) and (H_2) are examined. For the non-infected compartments, the reduced system is obtained as

$$F(X_r,0)=\begin{pmatrix}\pi-\mu S\\ -\mu R\end{pmatrix}. \tag{16}$$

The solutions are given by

$$S(t)=\frac{\pi}{\mu}+\left(S(0)-\frac{\pi}{\mu}\right)e^{-\mu t},$$

and

$$R(t) = R(0)e^{-\mu t}.$$

Hence, as $t \to \infty$,

$$S(t) \to \frac{\pi}{\mu}, \qquad R(t) \to 0,$$

which shows that condition (H_1) is satisfied.

For condition (H_2), let

$$Z = (E, I, I_R)^T.$$

The nonlinear part is expressed as

$$G(X,Z) = \begin{pmatrix} \frac{\beta(I+\rho I_R)S}{N} + \frac{\beta(1-\psi)(I+\rho I_R)R}{N} - (\kappa+\mu)E \\ \kappa E - (\tau+\sigma+\delta_1+\mu)I \\ \sigma I - (\eta+\delta_2+\mu)I_R \end{pmatrix}. \tag{17}$$

Following the decomposition,

$$\hat{G}(X,Z) = PZ - G(X,Z),$$

we obtain

$$\hat{G}(X,Z) = \begin{pmatrix} -\frac{\beta(1-\psi)(I+\rho I_R)R}{N} \\ 0 \\ 0 \end{pmatrix}.$$

Since the first component is non-positive, condition (H_2) is not satisfied. Therefore, the sufficient conditions for global asymptotic stability are not satisfied, and further analysis such as center manifold theory or bifurcation analysis is required to determine the possibility of backward bifurcation.

3.3 Endemic Equilibrium Point of TFE

The endemic equilibrium is obtained as

$$(S^*, E^*, I^*, I_R^*, R^*) = \left\{ \frac{\pi}{\lambda+\mu}, \frac{d_1(n_4\lambda^2+n_5\lambda)}{\kappa(n_1\lambda^2+n_2\lambda+n_3)}, \frac{n_4\lambda^2+n_5\lambda}{n_1\lambda^2+n_2\lambda+n_3}, \right.$$
$$\left. \frac{\sigma(n_4\lambda^2+n_5\lambda)}{d_2(n_1\lambda^2+n_2\lambda+n_3)}, \frac{d_4(n_4\lambda^2+n_5\lambda)}{(d_2d_3\lambda+d_2\mu)(n_1\lambda^2+n_2\lambda+n_3)} \right\}.$$

A bi-quadratic polynomial equation is created from the endemic equilibrium condition by substituting the above equation into (1) and equating it to zero, as follows.

$$\xi_1\lambda^4 + \xi_2\lambda^3 + \xi_3\lambda^2 + \xi_4\lambda + \xi = 0 \tag{18}$$

where,

$$\xi_1 = d_1 d_2^2 d_3 n_4 + \kappa d_2^2 d_3 n_4 + \kappa\sigma d_2 d_3 n_4,$$

$$\begin{aligned}\xi_2 = {} & \pi\kappa d_2^2 d_3 n_1 + \mu d_1 d_2^2 n_4 + d_1 d_2^2 d_3 n_5 + \mu d_1 d_2^2 d_3 n_4 + \kappa\mu d_2^2 n_4 \\ & + \kappa d_2^2 d_3 n_5 + \kappa q d_2^2 d_3 n_4 + \kappa\sigma u d_2 n_4 + \kappa\sigma d_2 d_3 n_5 \\ & + \kappa\sigma\mu d_2 d_3 n_4 + \kappa d_2 d_4 n_4 - \beta\kappa\Upsilon_1 d_2 d_3,\end{aligned}$$

$$\begin{aligned}\xi_3 = {} & \pi\kappa\mu d_2^2 n_1 + \pi\kappa d_2^2 d_3 n_2 + \mu d_2^2 d_1 n_5 + \mu^2 d_2^2 d_1 n_4 \\ & + \mu d_2^2 d_1 d_3 n_5 + \kappa u d_2^2 n_5 + \kappa\iota^2 d_2^2 n_4 + \kappa u d_2^2 d_3 n_5 \\ & + \kappa\sigma\mu^2 d_2 n_4 + \kappa\sigma\mu d_2 n_5 + \kappa\sigma\mu d_2 d_3 n_5 + \kappa d_2 d_4 n_5 \\ & + \kappa u d_2 d_4 n_4 - \beta\kappa\left(\Upsilon_1 d_2\mu + \Upsilon_2 d_2 d_3 + \Upsilon_1\mu d_2 d_3\right),\end{aligned}$$

$$\begin{aligned}\xi_4 = {} & \pi\kappa u d_2^2 d_3 n_3 + \pi\kappa d_2^2 d_3 n_3 + \mu^2 d_2^2 d_1 n_5 + \kappa\sigma\mu^2 d_2 n_5 \\ & + \kappa u d_2 d_4 n_5 - \beta\kappa\left(\Upsilon_1 d_2\mu^2 + \Upsilon_2 d_2\mu + \Upsilon_2\mu d_2 d_3\right),\end{aligned}$$

$$\xi_5 = \pi\kappa\iota^3(\eta + \delta_2 + \mu)^3(\tau + \sigma + \delta_1 + \mu)(\kappa + \mu)(1 - R_0).$$

Following the method applied in [8,18-21], it can easily be seen from (19) that $\xi_1 > 0$ (given that none of the model's inputs are negative). Additional, $\xi_5 < 0$ whenever $R_0 < 0$. According to the signs of ξ_2, ξ_3 and ξ_4, the polynomial (18) can thus have no number of possible positive real roots. Thus, the polynomial maximum number of positive real roots relies on the signs of ξ_2, ξ_3 and ξ_4. This can be examined using the quartic Descartes Rule of Signs.

Let $g(x) = \xi_1\lambda^4 + \xi_2\lambda^3 + \xi_3\lambda^2 + \xi_4\lambda + \xi_5$. Table 2 lists the numerous root-possibilities for the variable $g(x)$. The numerous options listed in Table 2 lead to the following conclusions.

Theorem 6. The tuberculosis disease model (1)

(i) If $R_0 > 1$ and any of Cases 1, 2, 3, and 6 are satisfied, the system has a distinct endemic equilibrium.

(ii) If $R_0 > 1$ and Cases 4, 5, 7, and 8 are satisfied, there may exist more than one endemic equilibrium.

(iii) If $R_0 < 1$ and Cases 2–8 are satisfied, there may exist two or more endemic equilibria.

3.4 Bifurcation Analysis

The objective of this section is to investigate the existence of backward bifurcation in system (1). This analysis is performed by applying the results presented in [17]. Based on the basic reproduction number, β is selected as the bifurcation parameter. By considering the threshold condition $R_0 = 1$, the critical value of β is obtained as

$$\beta^* = \frac{(\kappa + \mu)(\tau + \sigma + \delta_1 + \mu)(\eta + \delta_2 + \mu)}{\kappa(\eta + \delta_2 + \mu + \rho\sigma)}.$$

Table 2: Number of possible positive real roots of $g(x)$ for $R_0 < 1$ and $R_0 > 1$

Case	ξ_1	ξ_2	ξ_3	ξ_4	ξ_5	R_0	No. of sign chance	Number of possible positive real roots (endemic equilibrium)
1	+	+	+	+	+	$R_0 < 1$	0	0
	+	+	+	+	-	$R_0 > 1$	1	1
2	+	-	-	-	+	$R_0 < 1$	2	2,0
	+	-	-	-	-	$R_0 > 1$	1	1
3	+	+	-	-	+	$R_0 < 1$	2	2,0
	+	+	-	-	-	$R_0 > 1$	1	1
4	+	-	+	-	+	$R_0 < 1$	4	4,2,0
	+	-	+	-	-	$R_0 > 1$	3	3,1
5	+	-	-	+	+	$R_0 < 1$	2	2,0
	+	-	-	+	-	$R_0 > 1$	3	3,1
6	+	+	+	-	+	$R_0 < 1$	2	2,0
	+	+	+	-	-	$R_0 > 1$	1	1
7	+	+	-	+	+	$R_0 < 1$	2	2,0
	+	+	-	+	-	$R_0 > 1$	3	3,1
8	+	-	+	+	+	$R_0 < 1$	2	2,0
	+	-	+	+	-	$R_0 > 1$	3	3,1

For simplicity, let $(S, E, I, I_R, R) = (x_1, x_2, x_3, x_4, x_5)$, where $X = (x_1, x_2, x_3, x_4, x_5)^T$ and $f = (f_1, f_2, f_3, f_4, f_5)^T$. Thus, system (1) can be rewritten as

$$F(X) = \begin{pmatrix} \pi - \left(\frac{\beta(x_3+\rho x_4)}{N} + \mu\right) x_1 \\ \frac{\beta(x_3+\rho x_4)x_1}{N} + \frac{\beta(1-\psi)(x_3+\rho x_4)x_5}{N} - (\kappa+\mu)x_2 \\ \kappa x_2 - (\tau+\sigma+\delta_1+\mu)x_3 \\ \sigma x_3 - (\eta+\delta_2+\mu)x_4 \\ \tau x_3 + \eta x_4 - \left(\frac{\beta(1-\psi)(x_3+\rho x_4)}{N} + \mu\right) x_5 \end{pmatrix} = \begin{pmatrix} f_1 \\ f_2 \\ f_3 \\ f_4 \\ f_5 \end{pmatrix}.$$

The Jacobian matrix evaluated at the disease-free equilibrium E_0 is given by

$$J(E_0) = \begin{pmatrix} -\mu & 0 & -\beta & -\beta\rho & 0 \\ 0 & -(\kappa+\mu) & \beta & \beta\rho & 0 \\ 0 & \kappa & -(\tau+\sigma+\delta_1+\mu) & 0 & 0 \\ 0 & 0 & \sigma & -(\eta+\delta_2+\mu) & 0 \\ 0 & 0 & \tau & \eta & -\mu \end{pmatrix}.$$

At the threshold value $\beta = \beta^*$, the Jacobian matrix $J(E_0)$ has a simple zero eigenvalue. The corresponding right and left eigenvectors are denoted by W and V, respectively, where

$$W = \Bigg(-\frac{\beta\kappa W_2(\eta+\delta_2+\mu+\rho\sigma)}{\mu(\tau+\sigma+\delta_1+\mu)(\eta+\delta_2+\mu)}, W_2, \frac{\kappa W_2}{\tau+\sigma+\delta_1+\mu}, \\ \frac{\kappa\sigma W_2}{(\tau+\sigma+\delta_1+\mu)(\eta+\delta_2+\mu)}, \frac{\kappa W_2((\eta+\delta_2+\mu)\tau+\sigma\eta)}{\mu(\tau+\sigma+\delta_1+\mu)(\eta+\delta_2+\mu)} \Bigg)$$

and

$$V = \left(0, V_2, \frac{(\kappa+\mu)V_2}{\kappa}, \frac{\beta\rho V_2}{\eta+\delta_2+\mu}, 0\right).$$

Following the approach introduced in [6], the coefficients determining the direction of bifurcation are given by

$$a = \sum_{k,i,j=1}^{5} v_k w_i w_j \frac{\partial^2 f_k}{\partial x_i \partial x_j}(0,0),$$

and

$$b = \sum_{k,i=1}^{5} v_k w_i \frac{\partial^2 f_k}{\partial x_i \partial \beta}(0,0).$$

The non-zero second-order partial derivatives are evaluated at the disease-free equilibrium, and the coefficients are obtained as

$$a = \frac{V_2 W_2 \beta\kappa(1-\psi)\Sigma_1}{\pi(\tau+\sigma+\delta_1+\mu)(\eta+\delta_2+\mu)}$$

and

$$b = \frac{V_2 W_2 \kappa(\rho+1)\Sigma_2}{\pi(\tau+\sigma+\delta_1+\mu)(\eta+\delta_2+\mu)}$$

where

$$\Sigma_1 = \mu(\eta+\delta_2+\mu) + \mu\sigma\rho + (\eta+\delta_2+\mu+\rho\sigma)(1+\rho),$$

and

$$\Sigma_2 = \mu(\eta+\delta_2+\mu)(\tau+\sigma+\delta_1+\mu+1) + \mu\sigma + (\eta+\delta_2+\mu)\tau + \sigma\eta - \beta(\eta+\delta_2+\mu+\rho\sigma).$$

The bifurcation coefficients a and b determine the direction of the bifurcation near the disease-free equilibrium. The signs of these coefficients determine whether the system undergoes a forward or backward bifurcation at $R_0 = 1$. The corresponding bifurcation diagram is presented in Figure 2, which provides a graphical illustration of the bifurcation behavior of the proposed tuberculosis model.

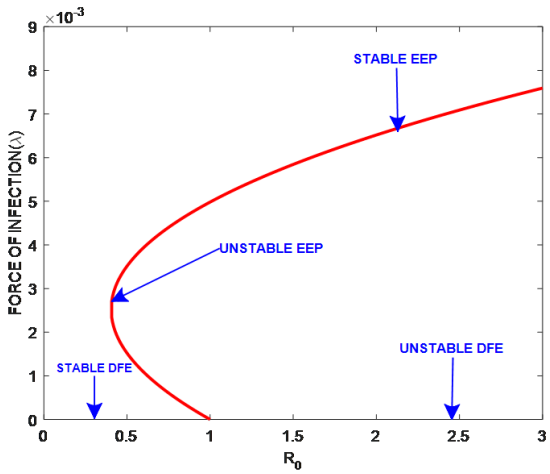

Figure 2: The force of infection against R_0 bifurcation diagram illustrating backward bifurcation in the system

3.5 Stability of endemic equilibrium on a global scale

Theorem 7. If $R_0 > 1$, the endemic equilibrium E_0^e of the model is globally asymptotically stable.

Proof: Determining a Lyapunov's function, L allows us to demonstrate the above theorem using the direct technique of Lyapunov and the invariant principle of LaSalle. We have

$$\begin{aligned} L(S^*, E^*, I^*, I_R^*, R^*) = &\left(S - S^* - S^* \ln \frac{S}{S^*}\right) + \left(E - E^* - E^* \ln \frac{E}{E^*}\right) \\ &+ \left(I - I^* - I^* \ln \frac{I}{I^*}\right) + \left(I_R - I_R^* - I_R^* \ln \frac{I_R}{I_R^*}\right) \\ &+ \left(R - R^* - R^* \ln \frac{R}{R^*}\right). \end{aligned}$$

Differentiating L with respect to t produces

$$\frac{dL}{dt} = \frac{(S - S^*)}{S}\frac{dS}{dt} + \frac{(E - E^*)}{E}\frac{dE}{dt} + \frac{(I - I^*)}{I}\frac{dI}{dt} + \frac{(I_R - I^*)}{I_R}\frac{dS}{dt} + \frac{(R - R^*)}{R}\frac{dR}{dt}.$$

Substituting the expressions for $\frac{dS}{dt}$, $\frac{dE}{dt}$, $\frac{dI}{dt}$, $\frac{dI_R}{dt}$, and $\frac{dR}{dt}$ into $\frac{dL}{dt}$ and simplifying, we obtain

$$\begin{aligned}
\frac{dL}{dt} &= \frac{S-S^*}{S}\big(\pi-(\lambda+\mu)S\big)+\frac{E-E^*}{E}\big(\lambda S+(1-\psi)\lambda R-(\kappa+\mu)E\big)\\
&\quad+\frac{I-I^*}{I}\big(\kappa E-(\tau+\sigma+\delta_1+\mu)I\big)\\
&\quad+\frac{I_R-I_R^*}{I_R}\big(\sigma I-(\eta+\delta_2+\mu)I_R\big)\\
&\quad+\frac{R-R^*}{R}\big(\tau I+\eta I_R-((1-\psi)\lambda+\mu)R\big)\\
&=\Bigg(\pi+\frac{S^*}{S}(\lambda+\mu)S+\frac{E^*}{E}(\kappa+\mu)E+\frac{I^*}{I}(\tau+\sigma+\delta_1+\mu)I\\
&\qquad+\frac{I_R^*}{I_R}(\eta+\delta_2+\mu)I_R+\frac{R^*}{R}\big((1-\psi)\lambda+\mu\big)R\Bigg)\\
&\quad-\Bigg(\mu S+\frac{S^*}{S}\pi+\mu E+\frac{E^*}{E}\lambda S+\frac{E^*}{E}(1-\psi)\lambda R\\
&\qquad+\delta_1 I+\mu I+\frac{I^*}{I}\kappa E+\delta_2 I_R+\mu I_R+\frac{I_R^*}{I_R}\sigma I\\
&\qquad+(1-\psi)\lambda R+\mu R+\frac{R^*}{R}\tau I+\frac{R^*}{R}\eta I_R\Bigg)\\
&= Z_1-Z_2.
\end{aligned}$$

where

$$\begin{aligned}
\mathbb{Z}_1 &= \pi+\frac{S^*}{S}(\lambda+\mu)S+\frac{E^*}{E}(\kappa+\mu)E+\frac{I^*}{I}(\tau+\sigma+\delta_1+\mu)I\\
&\quad+\frac{I_R^*}{I_R}(\eta+\delta_2+\mu)I_R+\frac{R^*}{R}\big((1-\psi)\lambda+\mu\big)R,\\
\mathbb{Z}_2 &= \mu S+\frac{S^*}{S}\pi+\mu E+\frac{E^*}{E}\lambda S+\frac{E^*}{E}(1-\psi)\lambda R\\
&\quad+\delta_1 I+\mu I+\frac{I^*}{I}\kappa E+\delta_2 I_R+\mu I_R+\frac{I_R^*}{I_R}\sigma I\\
&\quad+(1-\psi)\lambda R+\mu R+\frac{R^*}{R}\tau I+\frac{R^*}{R}\eta I_R,
\end{aligned}$$

$$\frac{dL}{dt}<0, \text{if } \mathbb{Z}_1<\mathbb{Z}_2,$$

$$\frac{dL}{dt}=0, \text{if and only if } S=S^*,\ E=E^*,\ I=I^*,\ I_R=I_R^*,\ R=R^*.$$

Hence, the largest invariant impact set within $(S^*, E^*, I^*, I_R^*, R^*) \in \Omega : \dfrac{dL}{dt} = 0$ is the individual element set E_0^* , where in E represents the endemic equilibrium of system (1). Consequently, according to the Invariant principle of Lasalle, as mentioned in [14], it can be deduced that E_0^* achieves global asymptotic stability within $\mathbb{Z}_1$ when Y is smaller than $\mathbb{Z}_2$.

3.6 Sensitivity Analysis

It is crucial to find out how responsive the changes in each of the parameters of the TB model (1) are expected in order to develop control measures that will help shorten the infection trajectory. To halt the propagation of tuberculosis, it will be helpful to undertake sensitivity analysis to determine what steps should be taken or not performed. [21, 22]. To help curb the spread of TB, sensitivity analysis will help determine whether measures should be followed or skipped. Applying the methodology in [23, 24], the normalized forward sensitivity index $\Gamma_t^{R_0}$ on the reproduction number R_0 for each of the parameters t, is defined as

$$\Gamma_t^{R_0} = \frac{\partial R_0}{\partial t} X \frac{t}{R_0} \tag{19}$$

In order to further illustrate the numerical outcome of the sensitivity indices, we offer a bar plot in Figure 3. It should be noted that any positive index from the sensitivity analysis would directly increase the threshold quantity of the disease and vice versa, whilst any negative index will cause a decrease in the threshold quantity and vice versa. From Figure 3, the parameters β, κ, ρ and σ demonstrate that increasing the values of these parameters raises R_0, this causes the infection to spread throughout the population. While the parameters $\eta, \tau, \delta_1, \delta_2$ and μ have negative values, increasing these parameters' levels, then, lowers the rate of reproduction, which causes the infection to eventually disappear from the population.The infection gradually dissipates in the population.

Besides, Table 3 shows the sensitivity index's largest negative value which is the rate of natural death. The findings shed light on control methods that are effective in reducing tuberculosis's population spread. For instance, the transition from exposed to actively infected κ has a positive index (+0.13081), which suggests that a 1% increase (or reduction) in κ value will result in a 1% increase (or decrease) in the number of reproductions. Additionally, the natural death index τ has a negative index of -0.89767, which means that a 1% change in τ value will result in a 1% change in the number of reproductions. The tuberculosis sensitivity analysis results, in summary, demonstrate the efficacy of any control methods that reduce the risk of transmission and the time it takes for a community to transition from exposure to active infection. Vaccination and therapy are two examples of this type of control mechanism, and they can be promoted through educational initiatives.

The outcomes listed in Table 3 shed light on effective strategies for managing the proliferation of multidrug resistant (MDR) tuberculosis (TB) within the community. For instance, when examining the transmission probability (β) a positive index of +1 indicates that a 1% increase (or decrease) in β' value leads to an equivalent 1% rise (or decline) in the reproduction number. Similarly, the negative index of -0.13081 associated with natural death (μ) signifies that a 1% rise (or drop) in μ' value corresponds to a 1% decrease (or increase) in the reproduction number.

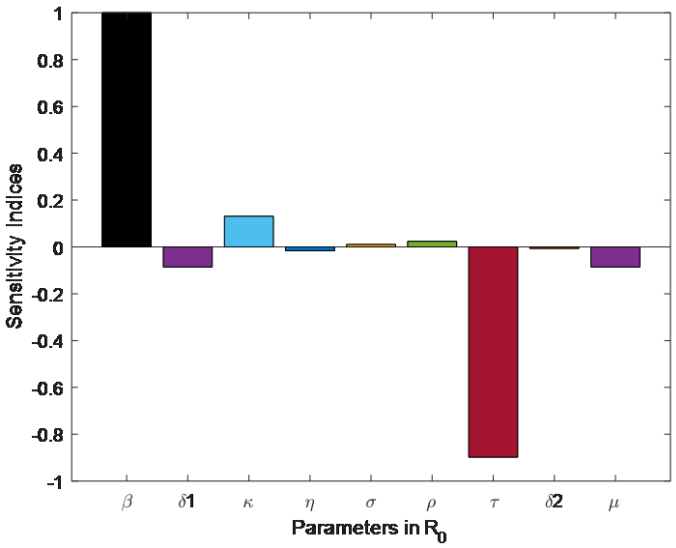

Figure 3: Sensitivity indices of the tuberculosis reproduction number R_0

Table 3: Normalized reproduction number sensitivity index

Parameter	Description	Sensitivity index	Sign
β	Transmission Rate	1	+ve
κ	The rate at which the exposed class advances to become the primary infectious class	0.13081	+ve
ρ	Modification parameters associated with drug resistance in individuals	0.02345	+ve
σ	Progression rate of primary infectious individuals into the drug-resistance class	0.01058	+ve
η	Transitioning from the drug-resistant class to the recovered class	-0.01656	-ve
τ	Individuals' progression from the primary infectious class to the recovered class	-0.89767	-ve
δ_1	Death rate due to primary infectious TB individuals	-0.08528	-ve
δ_2	Disease-induced death rate because of resistance to the drug	-0.00629	-ve
μ	Natural death rate	-0.08528	-ve

In a nutshell, the sensitivity analysis conducted on TB demonstrates that strategies capable of diminishing transmission probabilities and reducing the influx of tuberculosis into the population can effectively curtail the propagation of TB among people. Illustrative examples of such control measures include vaccination campaigns, treatment interventions for actively infected individuals and educational initiatives. This implies that tackling TB' spread hinges on a combination of factors that contribute to reducing the transmission and raising awareness.

4 Numerical Simulation and Discussion

To investigate how TB spreads, we created a deterministic $SEII_RR$ model. The findings from our model analysis show that the model is appropriately posed mathematically and epidemiologically, with positive and bounded solutions. We investigated and computed the basic reproduction number and evaluated the stability of the equilibrium point. Based on Lyapunov's theory, our findings show that when $R_0 < 1$ is formed, the equilibrium point where tuberculosis illness is absent is globally asymptotically stable. By employing the Centre manifold theory, we conducted a bifurcation analysis on the model, revealing a backward bifurcation at $R_0 = 1$; this implies that when $R_0 < 1$, both a stable EE and a tuberculosis DFE co-exist. The occurrence of the model's backward bifurcation predicts that reducing the basic reproduction number below one alone cannot lead to the extinction of the disease.

The second phase of the analysis entailed assessing the sensitivity of the fundamental reproduction number's attributes. Positive sensitivity was observed for the transmission rate β, the modification parameters associated with drug-resistance individuals ρ, and the pace at which exposed people develop primary infectiousness κ. The basic reproduction number will increase as these parameters are increased. Therefore, to eradicate tuberculosis, reducing the values of these parameters is necessary. On the other hand, the rate at which primary infectious individuals are recovered τ, the rates of natural mortality μ, TB disease-related deaths due to primary infections δ_1, the rate of drug-resistance δ_2, and the recovery rate of drug-resistance η exhibited negative sensitivity. Increasing the values of these factors will result in a drop in the basic reproduction number.

In the third part of the analysis, the scaling factor of the transmission parameter was changed from 1.73 to 2.53. The corresponding results are presented in Figure 4. In Figure 4, various β values of are applied in the clockwise direction, changing as the bifurcation parameter β moves from top left to bottom right, $\beta = 2.53, \beta = 2.43, \beta = 2.33, \beta = 2.23$ and $\beta = 1.73$ while the values of the other parameters are fixed $\mu = 0.018, \eta = 0.5, \delta_1 = 0.19, \delta_2 = 0.91, \kappa = 0.1196, \rho = 0.85, \tau = 2.0$ and $\sigma = 0.02$. It is evident that when the transmission parameter values increase, the bifurcation diagram demonstrates backward bifurcation. When the value is equal to or less than 1.73, the model shows forward bifurcation, demonstrating that reducing the basic reproduction number to below one can eradicate the infection.

However, between these values, eradicating the disease becomes impossible. In addition, the scaling factor of the recovery of the drug-resistance parameter was modified from 0.5 to 1, and the outcomes are shown in Figure 5. The bifurcation parameter η changes from top left to the bottom right with $\eta = 0.5, \eta = 0.6, \eta = 0.7, \eta = 0.8, \eta = 0.9$ and $\eta = 1$ while the values the other parameters are fixed $\mu = 0.018, \beta = 2.53, \delta_1 = 0.19, \delta_2 = 0.19, \kappa = 0.1196, \rho = 0.85, \tau = 2.0$ and $\sigma = 0.02$. These figures indicate that as the values of the recovery of the drug-resistance parameter increase, the bifurcation diagram exhibits a forward ward bifurcation.

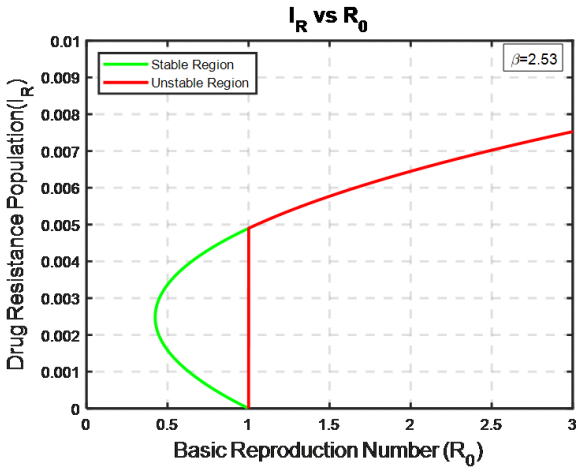

(a) Basic Reproduction Number (R_0) at $\beta = 2.53$

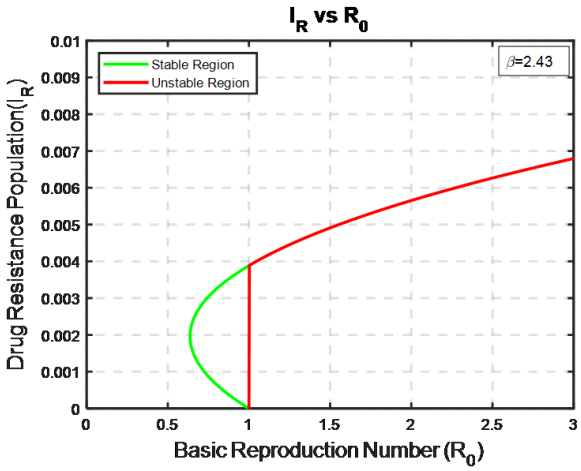

(b) Basic Reproduction Number (R_0) at $\beta = 2.43$

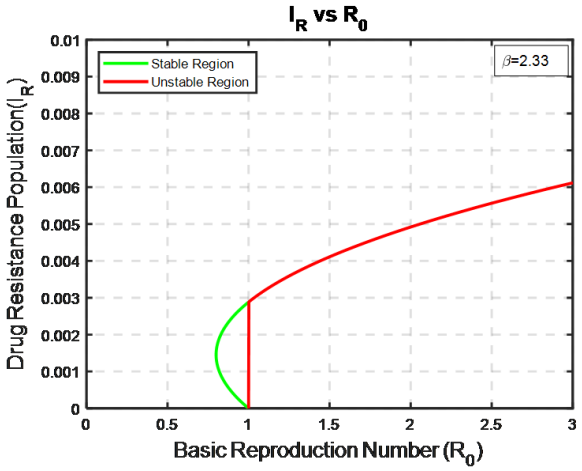

(c) Basic Reproduction Number (R_0) at $\beta = 2.33$

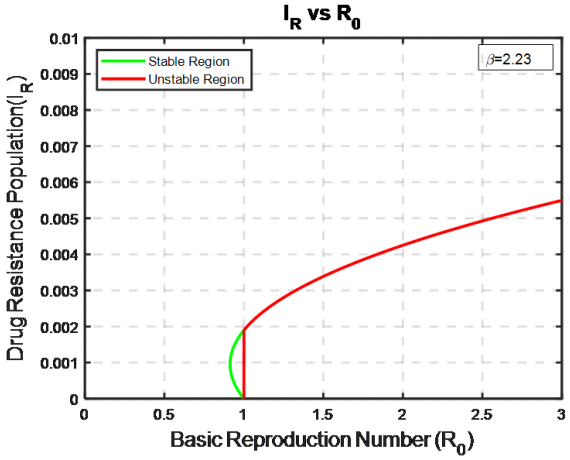

(d) Basic Reproduction Number (R_0) at $\beta = 2.23$

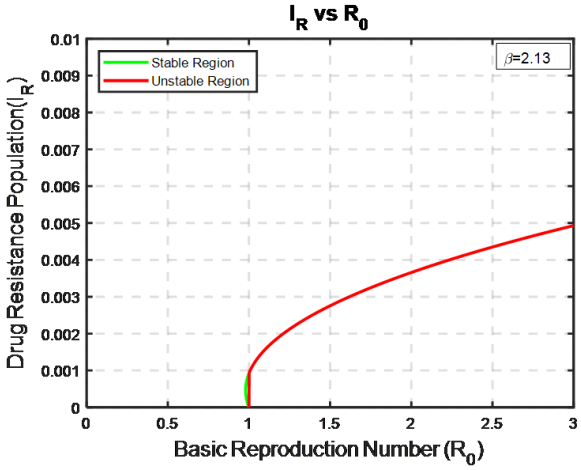

(e) Basic Reproduction Number (R_0) at $\beta = 2.13$

Figure 4: System model (1) backward bifurcation diagram displaying various behavior on transmission rates

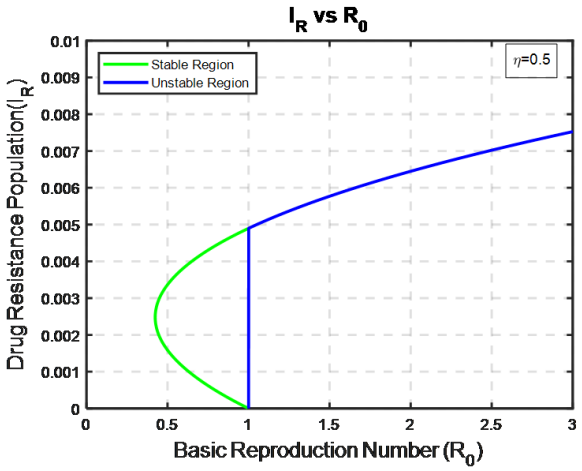

(a) Basic Reproduction Number (R_0) at $\eta = 0.5$

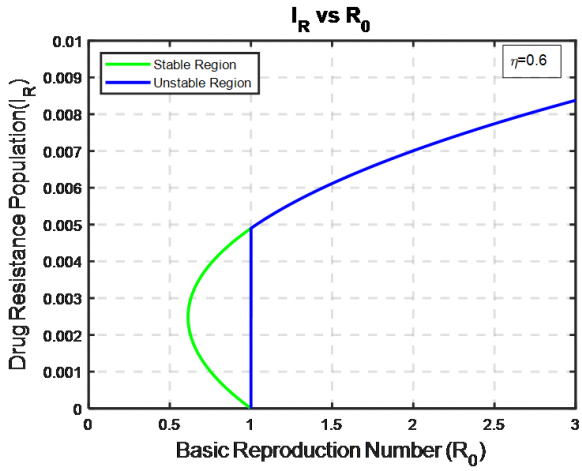

(b) Basic Reproduction Number (R_0) at $\eta = 0.6$

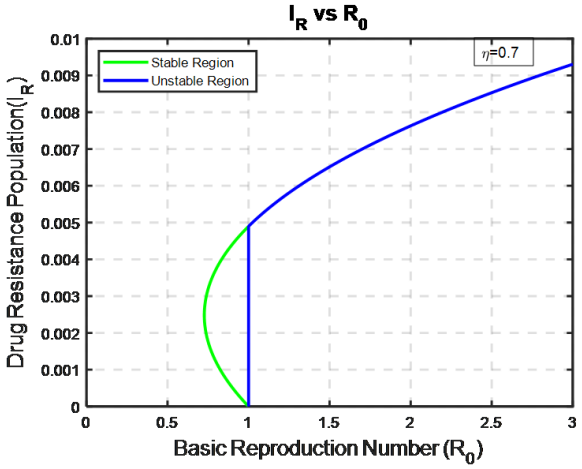

(c) Basic Reproduction Number (R_0) at $\eta = 0.7$

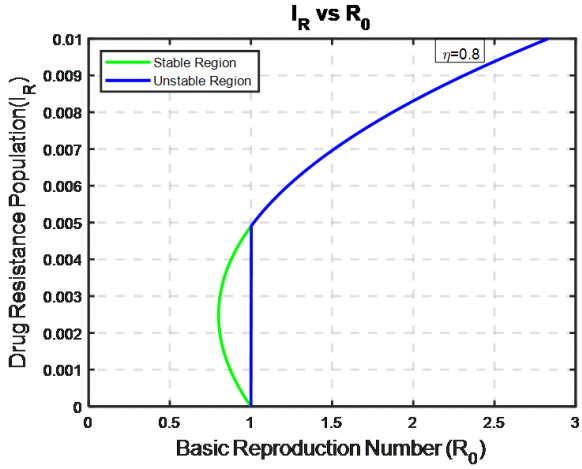

(d) Basic Reproduction Number (R_0) at $\eta = 0.8$

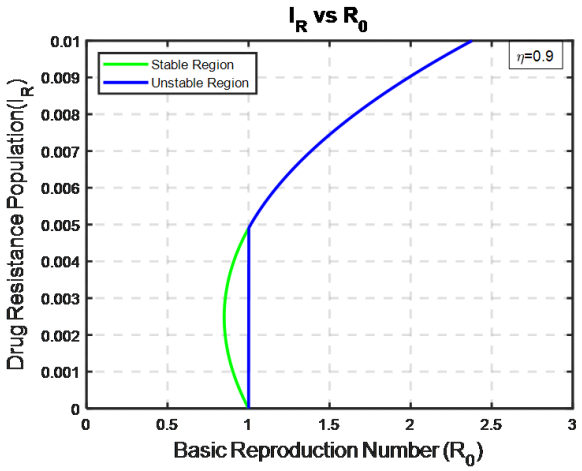

(e) Basic Reproduction Number (R_0) at $\eta = 0.9$

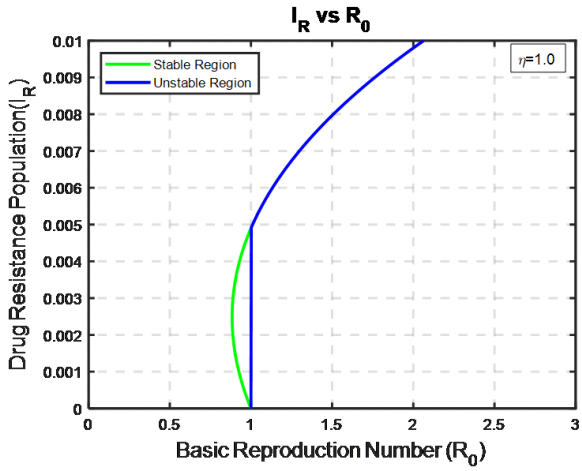

(f) Basic Reproduction Number (R_0) at $\eta = 1$

Figure 5: System model (1) backward bifurcation diagram displaying various behavior on recovery rate

We also investigated the impact of different parameters on the drug-resistance population within the model. Initially, we focused on the transmission scaling factor. As we increased the scaling factor of the transmission parameter from 1.73 to 2.53, we observed a decrease in the prevalence of drug-resistant individuals among the population. Next, we analyzed the contact rate and found that increasing the recovery rate of drug resistance from 0.5 to 0.9 reduced the population of individuals with drug resistance.

Figure 6(a) illustrates the impact of transmission rate (β) on the total number of infected individuals with DR as we vary $\beta = 2.53, 2.63, 2.73, 2.83, 2.93$. As β decreases, the peak becomes less pronounced and drastically reduced. It reveals that when the transmission rate of the disease is increased, on condition that the contact rate of the disease is kept minimal, the outbreak of the disease can be controlled. Figure 6(b) Illustrates the effect of the increasing recovery rate on the total number of infected individuals with drug-resistance as vary $\eta = 0.5, 0.6, 0.7, 0.8, 0.9, 2.93$. It reveals that when the recovery rate of the disease is increased, the highest value of η significantly reduced the spread of infection in a population.

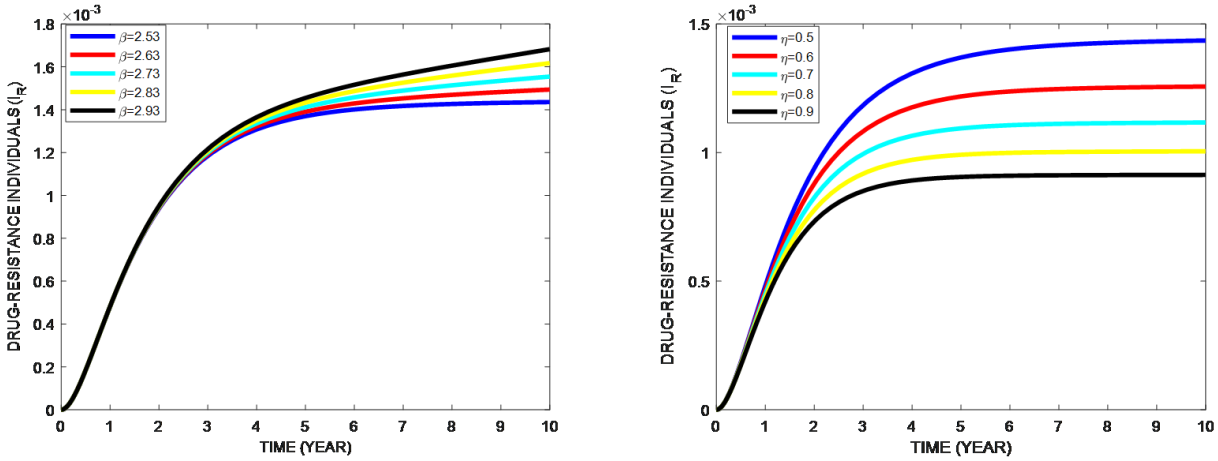

(a) Increased transmission rate **(b)** Increased recovery rate

Figure 6: Sensitivity analysis of the Drug-Resistance Population (I_R) to changes in transmission and recovery rates

On the other hand, from Figure 7(a), we observed that the population of susceptible individuals increased exponentially because of the influx of individuals into the population. Latently infected individuals with drug resistance decrease and rise gradually, as shown in Figure 7(b), failing treatment efficacy. From Figure 7(c), we observe that the population of primary infectious individuals increased exponentially before reaching to a steady point because of treatment efficacy. Similarly, in Figure 7(d), it was observed that the population of drug-resistant individuals increased exponentially and later remained at the same level because of treatment efficacy. Figure 7(e) shows that the population of recovered individuals also increased exponentially over time and later decreased slightly because both primary infectious individuals and individuals with drug resistance recovered as a result of proper treatment.

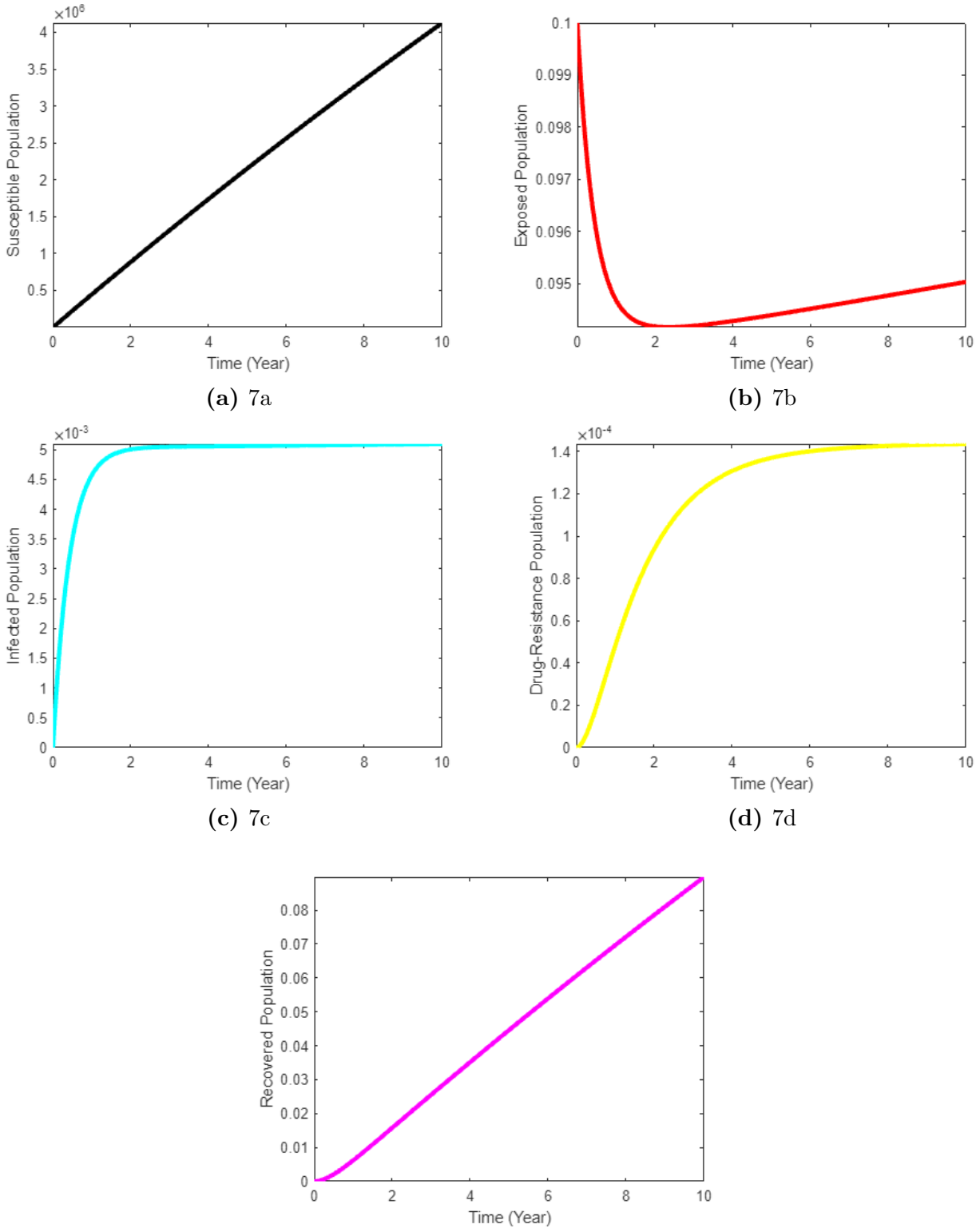

(a) 7a **(b)** 7b

(c) 7c **(d)** 7d

(e) 7e

Figure 7: The population for each compartment.

Finally, Figure 8 shows that both the primary infected (I_P) and drug-resistant infected (I_R) populations decrease continuously with time and eventually converge to zero, indicating the elimination of tuberculosis under the parameter values given in Table 1.

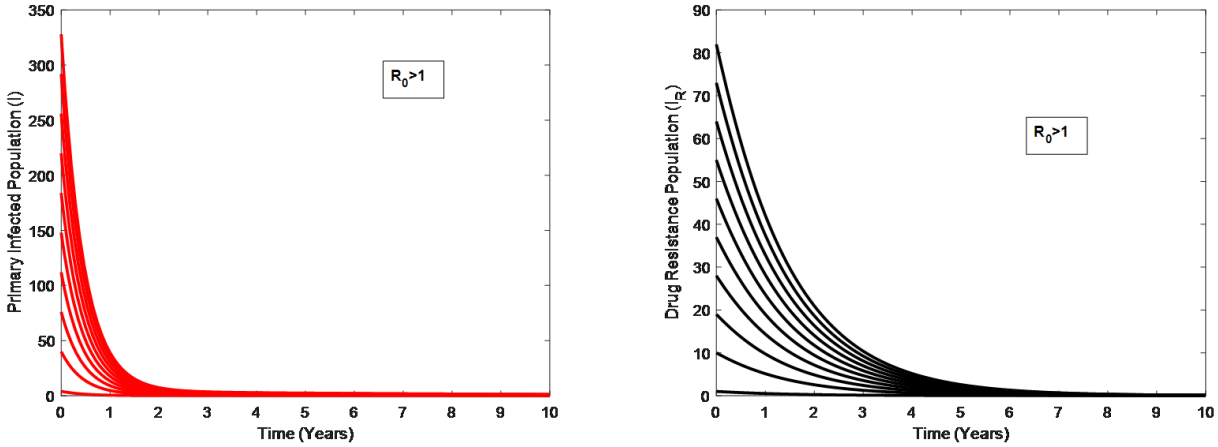

(a) Primary infected (I_P) **(b)** Drug-resistance infected (I_R)

Figure 8: Solution trajectories for entire population with parameter values listed in Table 1

5 Conclusions

The dynamic behavior of the drug-resistant and reinfected tuberculosis model was established in this work. It was demonstrated that the TB model is bounded. Additionally, the invariant region was found where the solutions of the basic TB model have biological importance. When the corresponding basic reproductive number $R_0 < 1$, the TB model with drug-resistance and reinfection in the TB-free situation is locally and globally asymptotically stable, according to mathematical study. Furthermore, the TB model with drug-resistance and reinfection is asymptotically stable both locally and globally when the corresponding basic reproductive number is maintained. If $R_0 < 1$, then TB infection will vanish; if not, it will remain common once Theorems 6 and 7 confirm the critical value needed to eradicate the illness. Using the center manifold theory, a thorough investigation of the TB model (1) reveals evidence for a backward bifurcation phenomenon, in which the equilibrium points for the endemic and disease-free states at exchange spots are stable.

Numerical investigations are performed to verify the theoretical results. It has been demonstrated that an increase in the rate of transmission leads to a significant force of infection. Furthermore, an increase in the rate of recovery may lead to a tremendous recovery of infected individuals in the population, even at a state of equilibrium. Future research can modify the model to incorporate various dynamics that influence the spread of TB infection. The dynamics of the tuberculosis (TB) model must be taken into account by incorporating an age-structured model, as the disease's transmission impacts individuals of all ages. Due to the difficulty of gathering data on TB patients in epidemiological models, we rely on information gleaned or deduced from sources in the literature. When we have real patient data on tuberculosis, we may compare it with expected outcomes. Additionally, in the future, we plan to enhance the

model described here by integrating the optimal control issue, applying Pontryagin's maximum principle. Because eradicating the disease in a large and underdeveloped population can be both severe and costly, we will conduct a cost-effectiveness analysis to determine the most cost-effective strategy among several combinations of control measures.

Acknowledgments

The authors express their heartfelt gratitude to the School of Mathematical Sciences at Universiti Sains Malaysia for providing them with access to the research resources necessary to carry out this study. With this acknowledgement, they are expressing their appreciation and acknowledging the support the institution provided them while they conducted their research.

References

[1] Kalu, A. U. and Inyama, S. C. Mathematical model of the role of vaccination and treatment on the transmission dynamics of tuberculosis, *Gen. Math. Notes*, 11(1) (2012), 10–23.

[2] Bhunu, C. P. and Garira, W. A two strain tuberculosis transmission model with therapy and quarantine, *Mathematical Modelling and Analysis*, 14(3) (2009), 291–312. DOI: `https://doi.org/10.3846/1392-6292.2009.14.291-312`.

[3] Nyerere, N., Luboobi, L. S. and Nkansah-Gyekye, Y. Modeling the effect of screening and treatment on the transmission of tuberculosis infections, *Mathematical Theory and Modeling*, 4(7) (2014), 51–63.

[4] World Health Organization. *Global Tuberculosis Report 2024*, World Health Organization, Geneva, 2024. Available at: `https://www.who.int/teams/global-tuberculosis-programme/tb-reports`.

[5] Wangari, I. M., Davis, S. and Stone, L. Backward bifurcation in epidemic models: Problems arising with aggregated bifurcation parameters, *Applied Mathematical Modelling*, 40 (2016), 1669–1675.

[6] Sulayman, F. and Abdullah, F. A. Dynamics of tuberculosis transmission model with reinfection issues, *Matematika*, 39(2) (2023), 125–148.

[7] Das, K., Murthy, B. S. N., Samad, S. A. and Biswas, M. H. A. Mathematical transmission analysis of SEIR tuberculosis disease model, *Sensors International*, 2 (2021), 100120. DOI: `https://doi.org/10.1016/j.sintl.2021.100120`.

[8] Mishra, B. K. and Srivastava, J. Mathematical model on pulmonary and multidrug-resistant tuberculosis patients with vaccination, *Journal of the Egyptian Mathematical Society*, 22(2) (2014), 311–316. DOI: `https://doi.org/10.1016/j.joems.2013.07.006`.

[9] Yeketi, A. A. and Othman, W. A. M. A compartmental model on the effect of quarantine on MDR-TB, *International Journal of Mathematics and Computer Science*, 14(3) (2019), 613–629.

[10] Sulayman, F., Abdullah, F. A. and Mohd, M. H. A SVEIRE model of tuberculosis to assess the effect of an imperfect vaccine and other exogenous factors, *Mathematics*, 9(4) (2021), 327. DOI: https://doi.org/10.3390/math9040327.

[11] Ishaku, A., Gazali, A. M., Abdullahi, S. A. and Hussaini, N. Analysis and optimal control of an HIV model based on CD4 count, *Journal of Mathematical Biology*, 81(1) (2020), 209–241. DOI: https://doi.org/10.1007/s00285-020-01508-8.

[12] Sulayman, F. and Abdullah, F. A. Dynamical behaviour of a modified tuberculosis model with impact of public health education and hospital treatment, *Axioms*, 11(12) (2022), 723. DOI: https://doi.org/10.3390/axioms11120723.

[13] Miller, B. Preventive therapy for tuberculosis, *Medical Clinics of North America*, 77(6) (1993), 1263–1275. DOI: https://doi.org/10.1016/S0025-7125(16)30192-4.

[14] Hale, J. K. and Lunel, S. M. V. *Introduction to Functional Differential Equations*, Springer, Berlin, 1993.

[15] Yusuf, T. T. and Abidemi, A. Effective strategies towards eradicating the tuberculosis epidemic: An optimal control theory alternative, *Healthcare Analytics*, 3 (2023), 100131. DOI: https://doi.org/10.1016/j.health.2022.100131.

[16] Sulayman, F. and Abdullah, F. A. Dynamical behaviour of a modified tuberculosis model with impact of public health education and hospital treatment, *Axioms*, 11(12) (2022), 723. DOI: https://doi.org/10.3390/axioms11120723.

[17] Saputra, H. L., Darti, I. and Suryanto, A. Analysis of SVEIL model of tuberculosis disease spread with imperfect vaccination, *JTAM (Jurnal Teori dan Aplikasi Matematika)*, 7(1) (2023), 125–138. DOI: https://doi.org/10.31764/jtam.v7i1.11033.

[18] Ucakan, Y., Gulen, S. and Koklu, K. Analyzing tuberculosis in Turkey through SIR, SEIR and BSEIR mathematical models, *Mathematical and Computer Modelling of Dynamical Systems*, 27(1) (2021), 179–202. DOI: https://doi.org/10.1080/13873954.2021.1881560.

[19] Chitnis, N., Cushing, J. M. and Hyman, J. M. Bifurcation analysis of a mathematical model for malaria transmission, *SIAM Journal on Applied Mathematics*, 67(1) (2006), 24–45. DOI: https://doi.org/10.1137/050638941.

[20] Olaniyi, S., Obabiyi, O. S., Okosun, K. O., Oladipo, A. T. and Adewale, S. O. Mathematical modelling and optimal cost-effective control of COVID-19 transmission dynamics, *European Physical Journal Plus*, 135(11) (2020), 938. DOI: https://doi.org/10.1140/epjp/s13360-020-00954-z.

[21] Olaniyi, S. Dynamics of Zika virus model with nonlinear incidence and optimal control strategies, *Applied Mathematics and Information Sciences*, 12(5) (2018), 969–982. DOI: https://doi.org/10.18576/amis/120510.

[22] Castillo-Chavez, C. Dynamical models of tuberculosis and their applications, 2004. Available at: http://math.asu.edu/~mbe/.

[23] Faniran, T., Ali, A., Adewole, M. O., Adebo, B. and Akanni, O. O. Asymptotic behavior of tuberculosis between smokers and non-smokers, *Partial Differential Equations in Applied Mathematics*, 5 (2022), 100244. DOI: https://doi.org/10.1016/j.padiff.2021.100244.

[24] Faniran, T. S. and Adewole, M. O. Analysis of a cholera model with treatment noncompliance, *International Journal of Nonlinear Analysis and Applications*, 13(1) (2022), 29–43. DOI: https://doi.org/10.22075/IJNAA.2021.23626.2568.